A Discussion of Losses and Changes in the Characteristic Impedance of Finitely-Conducting Planar Transmission-Line Structures

Christopher L. Holloway

National Institute of Standards and Technology (NIST), 325 Broadway, Boulder, CO 80305, USA
Phone: (303)-497-6184, email: holloway@boulder.nist.gov

Abstract

This paper discusses the effects that imperfect conductors have on the propagation characteristics of planar transmission-line structures. We present closed-form expressions for the attenuation constant and the resistance per unit length for various planar structures are presented. We also present expressions for predicting the change in the characteristic impedance due to penetration of fields into finite conductors.

INTRODUCTION

The speed of processors is increasing each year, and has resulted in faster pulses on printed circuit board (PCB) transmission-line (TL) structures. Faster pulses imply high-frequency content propagating on the TL. High-frequency propagation characteristics of lossy (i.e., finite conducting metals) TLs can adversely affect signal integrity in high-speed digital lines. Hence, a serious need exists to understand and accurately characterize the propagation of high-frequency waveforms (narrow-pulse digital waveforms) on lossy transmission-line structures. This paper discusses propagation characteristics associated with finite conducting TLs.

EFFECTS OF FINITE CONDUCTIVITY

The distributed series impedance Z and shunt admittance Y per unit length of TL are defined as

$$\begin{aligned} Z &= R + j\omega L \\ Y &= G + j\omega C \end{aligned}, \qquad (1)$$

where R (W/m), L (H/m), C (F/m), and G (S/m) represent the series resistance, series inductance, shunt capacitance and shunt conductance per unit length (p.u.l.), respectively. In general, all four of the transmission-line parameters are frequency dependent. Of most interest in this paper are the finite conductivity effects, which generally affect R, L, and C. We will neglect the effects on C. L represents both the external and internal inductance. At dc, L is essentially the external plus the dc internal inductance. As the frequency increases, due to the well known "skin effect", the internal inductance decreases [1, 2, 3] and L approaches the external inductance. On the other hand, as the frequency increases, R increases from its dc value R_{dc} due to the decreasing of the effective cross section of the conductor. As the frequency increases from dc, the internal fields are forced toward the surface of the conductors and are no longer uniformly distributed in the conductor cross-section. This results in a $\sqrt{f}$ (where f is frequency) behavior in R and a $1/\sqrt{f}$ behavior in L [1-3].

This dispersive nature of the line parameters causes two adverse effects. The first is associated with pulse distortion due to loss, and the second is associated with the change in the characteristic impedance Z_o due to field penetration into the metals. Pulse distortion is discussed first. The time-domain high-speed digital waveforms alter their shape when propagating along a lossy TL. This is illustrated in Figure 1, which shows results both for accurately accounting for dispersion and for assuming only dc loss (i.e., no dispersion). The pulse on the lossy TL is broadened and exhibits the classic late-time tail, seen in time-domain response of lossy media. From this figure we also see that the dc approximation (i.e., dc losses only) does not correctly predict the pulse shape. The pulse obtained from the dc approximation is larger in amplitude and narrower in width. Notice however, that the two results in this figure approach the same late-time values. This is due to the fact that the late-time response corresponds to low frequency in the frequency domain, which the dc model captures. On the other hand, the early-time response (the front edge of the pulse), which corresponds to high frequency in the frequency domain, is where the two cases differ. This is due to the fact that the dc model cannot capture the high-frequency behavior of the TL. This illustrates the need to accurately characterize loss for signal integrity analysis.

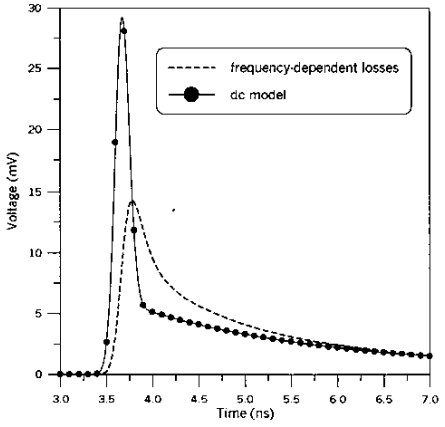

Figure 1: Output time-domain waveform for a lossy 0.5m long CPW line.

The second issue addressed in this paper is the effect of finite conductivity on the characteristic impedance Z_o. The Z_o of a TL changes as a function of frequency due to field penetration into the finite conductive metals, becoming large at low frequencies and monotonically approaching an asymptotic limit at high frequency. In this paper, we present expressions for predicting R p.u.l. for a finite conducting planar TLs. We will also present closed-form corrections (due to field penetration) for the characteristic impedances of planar TLs.

RESISTANCE p.u.l.

In previous work [4], the electromagnetic fields in the vicinity of an edge of a conducting strip have been investigated with a matched asymptotic-expansion technique. With this asymptotic solution of the fields, the power loss in the region local to the edge was determined accurately. It has been demonstrated that this accurate representation of the power loss near an edge can be used to obtain closed-form expressions for the conductor loss (i.e., the attenuation constant α) for planar structures [4-7]. With the expression for the attenuation constant given in [4-7], the resistance R p.u.l. is well approximated by

$$R_o \approx 2 Z_o \alpha \approx \frac{\mathrm{Re}[Z_{sm}]}{2} GF , \qquad (2)$$

where Z_{sm} is the modified Horton surface impedance [4]. This impedance boundary condition takes into account coupling from the top and bottom sides of the strip and is given by

$$Z_{sm} = j\sqrt{\frac{\mu_c}{\varepsilon_c}}\left[\cot(k_c t) + \csc(k_c t)\right] , \qquad (3)$$

where μ_c and ε_c are the permeability and permittivity, respectively, k_c is the complex wave-number in the medium, and t is the strip thickness. The geometric factor GF is a function of the geometry of the planar structure and is given for a microstrip and stripline (SL) by [4-7]:

$$GF_{\mu} = GF_{SL} = \frac{2}{w\pi^2}\ln\left(\frac{w}{\Delta}-1\right) , \qquad (4)$$

where w is the strip width. For coplanar waveguide (CPW) and coplanar strips (CPS) the corresponding expression is

$$GF_{CPW} = GF_{CPS} = \frac{b^2}{4\left(b^2-a^2\right)K^2(g)}\left\{\frac{1}{a}\ln\left(\frac{2a}{\Delta}\frac{b-a}{b+a}\right) + \frac{1}{b}\ln\left(\frac{2b}{\Delta}\frac{b-a}{b+a}\right)\right\} , \qquad (5)$$

where $K(g)$ is the elliptic integral of the first kind. For the CPW line a is one-half of the center conductor width, b is one-half of the total distance between ground planes, and $g = a/b$. For the CPS line, a is one-half the strip separation, b is the strip width plus one-half the separation, and $g = \sqrt{1-(a/b)^2}$. In these expressions for GF, Δ is a parameter referred to as the stopping distance and is a function of the strip thickness, the edge shape, and the conductor's properties. Values of Δ for normal conductors and superconductors are given in [5, 6].

Unfortunately, due to the inherent assumptions made in the derivation of this expression, R does not reduce to the dc limit. R varies monotonically from its dc value to the $\sqrt{f}$ behavior at higher frequency. Such a variation can be approximated by the following expression:

$$R = R_o + \left(R_{dc} - \frac{1}{t\sigma}GF\right)\exp^{(-2t/\delta)} , \qquad (6)$$

where R_o is given in equation (2) and R_{dc} is the dc resistance. This expression assures that R_{dc} is obtained for small values of the t/δ (where δ is the skin depth). A comparison of this expression to the measured data for a microstrip line is shown in Figure 2. This comparison differs by no more than 4%. Comparisons to other structures show similar or better correlation.

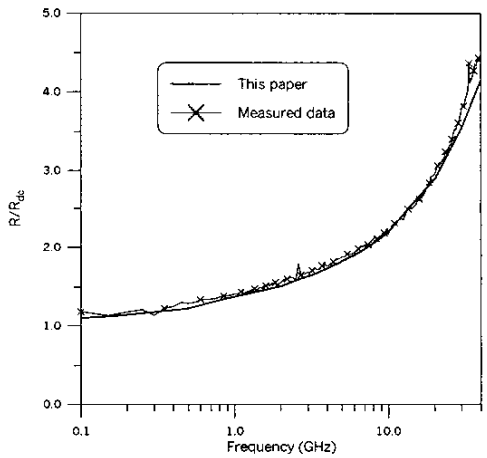

Figure 2: R for a microstrip line with w=105μm, t=1.8μm, h=254μm, σ=3.9x10^7 S/m and ε_r=10.

To further illustrate the accuracy of these expression, the attenuation constant obtained from equation (2) is compared to both measured [8, 9] and full-wave [10] results. Figures 3, 4, 5, and 6 show such comparisons for microstrip, strip-line, CPS and CPW structures, respectively. Once again, good correlation is demonstrated.

There are a few interesting things to notice in these four figures. Figure 3 shows results for two different width of microstrip lines. Notice that if the width of a microstrip line

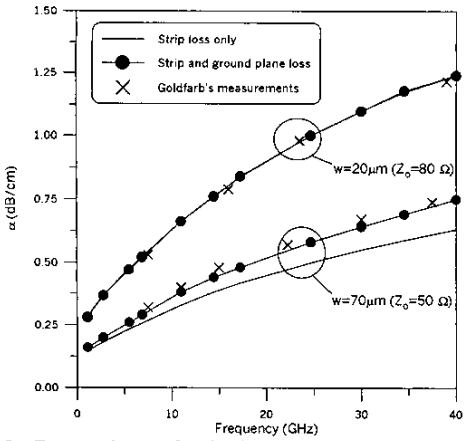

Figure 3: Comparison of calculated loss with measured data [8] for a microstrip with h=100μm, t=3μm, σ=4.1x10^{7}S/m, and ε_r=12.9.

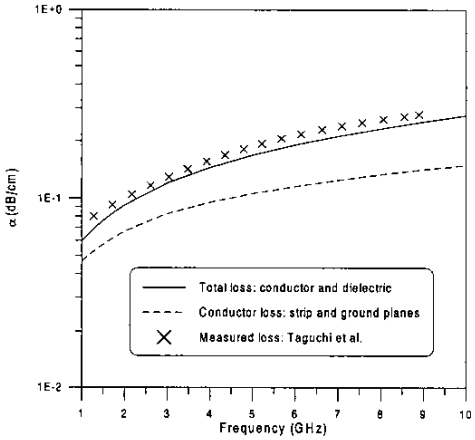

Figure 4: Comparison of calculated loss with measured data [9] for a strip-line with t=10μm, w=200μm, h=455μm, σ=2.5x10^7 S/m, ε_r=7.77, and tanδ=0.005.

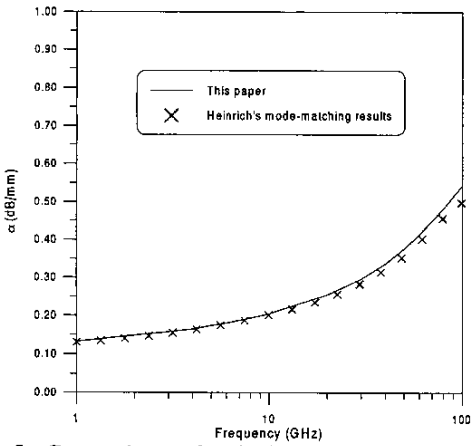

Figure 5: Comparison of calculated conductor loss with Heinrich's mode-matching approach for a CPS with t=1.5μm, a=10μm, b=25μm, σ=3.0x10^{7}S/m, and ε_r=12.9.

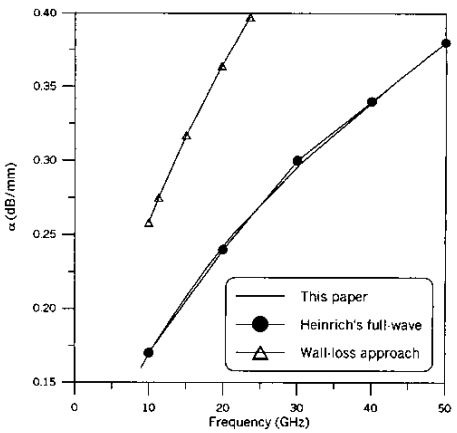

Figure 6: Comparison of calculated conductor loss with Heinrich's mode-matching approach [10] for a CPW with t=3μm, a=5μm, b=25μm, σ=3.0x10^{7}S/m, and ε_r=12.9.

becomes comparable to the height, loss associated with a finitely conducting ground plane approaches the loss of the strip; see [11, 12] for details. The same is true of SL structures, see [7].

The expressions given here are for conductor loss only; dielectric losses are not included. In some situations the dielectric loss can be significant and needs to be considered in the loss calculations. This is illustrated in Figure 4, where it is shown that for the particular structure investigated, dielectric loss is important. A discussion of dielectric loss can be found in [3] and in [13, 14].

The classic approach for determining conductor loss is the wall-loss perturbation approach based on Wheeler's incremental inductance rule. Figure 6 compares this wall-loss approach both to the expression presented here and to a full-wave result. The classical Wheeler's incremental inductance rule fails because the surface impedance used in Wheeler's rule does not account for the edge effects of the conductors (see [4]). The expressions presented here do account for edge effects.

Finally, with these expressions we can investigate how R changes with strip thickness t and with changes in the conductivity. Figure 7 shows R as a function of strip thickness t for two values of frequency. As expected, the loss is larger for the higher frequency. Furthermore, notice that R increases dramatically for $t < 1$ μm. This is due to the fact that cross-sectional area decreases and so the edge effects become more important for small t.

Figure 8 shows R as a function of frequency for two values of conductivity. As expected, the loss is higher for the smaller value of conductivity.

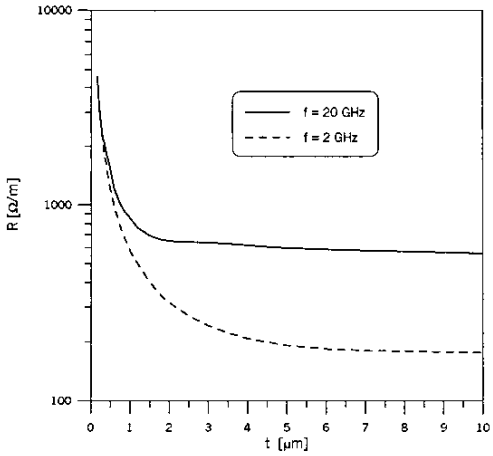

Figure 7: Variations in R as a function of strip thickness t for two values of frequency for a microstrip with w=70μm, h=100μm, t=3μm, and σ=3.6x10^{7}S/m.

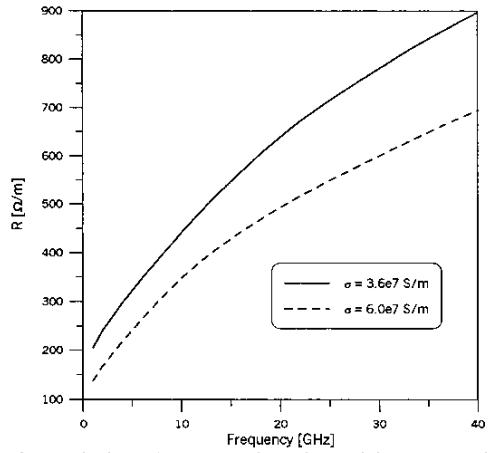

Figure 8: Variations in R as a function of frequency for two values of conductivity for a microstrip with w=70μm, h=100μm, and t=3μm.

CHANGES IN CHARACTERISTIC IMPEDANCE

The standard expressions used for the characteristic impedance for CPW, CPS, and SL structures are given by [15] and [16]

$$Z_{o,CPW} = \frac{120\pi}{4\sqrt{\varepsilon_{eff}}}\frac{K(g')}{K(g)}$$

$$Z_{o,CPS} = \frac{120\pi}{\sqrt{\varepsilon_{eff}}}\frac{K(g)}{K(g')} \quad , \qquad (7)$$

$$Z_{o,SL} = \frac{120\pi}{4\sqrt{\varepsilon_r}}\frac{K(g)}{K(g')}$$

where g for CPW and CPS were defined previously, $g = \sec h[\pi w/(4h)]$ for SL, and $g' = \sqrt{1-g^2}$ for all three cases. For CPW and CPS $\varepsilon_{eff} = (\varepsilon_r + 1)/2$ in (7). The characteristic impedance of a microstrip line is approximated with an accuracy of 2 % or better by [17]

$$Z_0 = 30\sqrt{\frac{2}{\varepsilon_r + 1}}\ln\left\{1 + \frac{32h}{w}\left[\frac{hr_\varepsilon}{w} + \sqrt{\left(\frac{hr_\varepsilon}{w}\right)^2 + \frac{\varepsilon_r + 1}{2}\left(\frac{\pi}{8}\right)^2}\right]\right\}, \qquad (8)$$

where $r_\varepsilon \cong \sqrt{0.4052 + 0.5160/\varepsilon_r + 0.0788/\varepsilon_r^2}$.

The equations in (7) and (8) are valid for perfectly conducting infinitely thin strips. For high-frequency applications, where there is little field penetration into the conducting strips, these two expressions give valid results. However, when the frequency decreases or the material properties of the conducting strip are such that the fields penetrate into the strip, these expressions break down. An accurate representation of the fields that penetrate into the conducting strip allows us to develop corrections for Z_o.

In previous work [4], the fields in the vicinity of an edge of a conducting strip have been investigated with a matched asymptotic technique. Extending this work, corrections to the characteristic impedance of any planar structure can be developed with the following procedure. Inside the conducting strips the electric fields are zero to zeroth-order, and the dominant fields in the conductor are magnetic [4]. The presence of the imperfect conductor will change only the inductance of the line; the capacitance is unchanged from that of a perfect conductor. Thus, the characteristic impedance of a quasi-TEM mode can be approximated by

$$Z_c = \sqrt{\frac{L_o}{C_o}}\sqrt{\frac{L}{L_o}} = Z_o\frac{\gamma_m}{\gamma_{mo}}, \qquad (9)$$

where Z_o is the characteristic impedance for a perfectly conducting infinitely thin structure [given in (7) and (8)], γ_m is the propagation constant for a finite conductor of thickness t, and γ_{mo} is the propagation constant for a perfectly conducting infinitely thin structure, given by $\gamma_{mo} = jk_o\sqrt{\varepsilon_{eff}}$. We have, however, neglected the change of C_o and L_o when the thickness changes from $t = 0$ to $t \neq 0$.

It is tempting to determine the change in the propagation constant by using standard perturbation methods; however this approach will fail due to the fact that the edge effects cannot be accounted for in a standard surface-impedance boundary condition. By assuming the conductors are infinitely thin, an approximate current density on the strips could be obtained and the stopping-distance idea can then be used to develop the following expression:

$$\gamma_m - \gamma_{mo} \approx \frac{1}{Z_c}\frac{Z_{sm}}{4}GF = \frac{1}{Z_o}\frac{\gamma_{mo}}{\gamma_m}\frac{Z_{sm}}{4}GF \quad , \qquad (10)$$

where GF is the geometric factor given in eqs. (4) and (5). Using equations (9) and (10), the characteristic impedance due to fields penetrating into the conductor is given by

$$Z_c = Z_o\left[1+\frac{Z_{sm}\,GF}{j4\,k_o Z_o\sqrt{\varepsilon_{eff}}}\right]\frac{1}{\sqrt{1+\dfrac{Z_{sm}\,GF}{j\,k_o Z_o\sqrt{\varepsilon_{eff}}}}} \quad . \qquad (11)$$

Figures 9 and 10 show the corrected characteristic impedance calculated from (11) for a CPW and microstrip line, respectively. In these figures, experimental results ([18] and [19]) for the characteristic impedances are also shown. Good correlation between the present theory and experimental results is demonstrated. Note that the correction [the second term in (11)] approaches zero in the high-frequency limit, so asymptotic limits in Figures 9 and 10 are Z_o. We should also note that, due to the approximations made here, equation (11) will break down at very low frequencies.

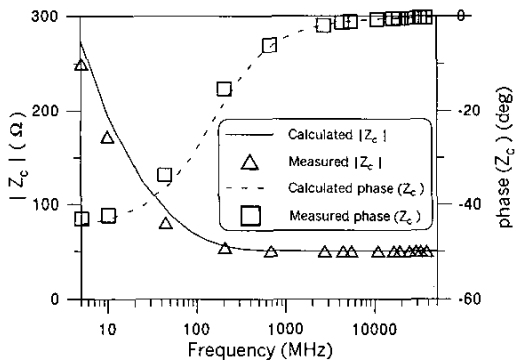

Figure 9: Characteristic impedance for a CPW line with t=1.6μm, a=36μm, b=85μm, σ=3.6x10^{7}S/m, and ε_r=12.9.

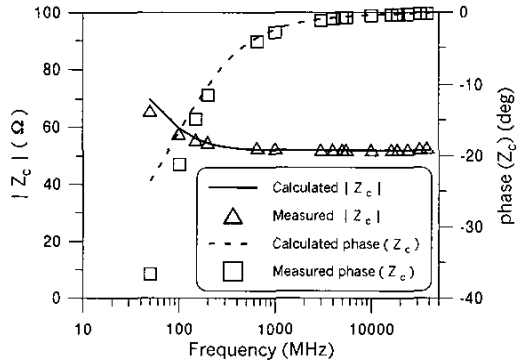

Figure 10: Characteristic impedance for a microstrip with w=75μm, h=110μm, t=1.6μm, σ=4.0x10^{7}S/m, and ε_r=12.9.

CONCLUSION

In this paper we presented a closed-form expression for determining the resistance (R) p.u.l. for various planar structures. These expressions have been compared to both measured and full-wave solutions, and good correlation is demonstrated. We also presented closed-form corrections for the characteristic impedances of planar structures that account for the field penetration inside the conducting strips. The expression for Z_o compares very well to experimental results. The finite-conductivity effects discussed in this paper are important and may need to be considered when designing high-speed digital lines.

REFERENCES

[1] C.R. Paul, *Analysis of Multiconductor Transmission lines*. N.Y.:John Wiley & Sons, 1994.

[2] P. Magnusson, G.C. Alexander, V.K. Tripathi, *Transmission lines and wave propagation*. Boca Raton, FL: CPR Press, 1992.

[3] J. Baker-Jarvis, M.D. Janezic, B. Riddle, C.L. Holloway, and N.G. Paulter, "Dielectric and conductor-loss characterization and measurements on electronic packaging materials," *NIST Technical Note 1520*, Boulder, CO, July 2001.

[4] C.L. Holloway and E.F. Kuester, *Radio Science*, 29(3), 539-559, 1994.

[5] C.L. Holloway and E.F. Kuester, *IEEE Trans. on MTT*, 43(12), 2695-2701, 1995.

[6] J.C. Booth and C.L. Holloway, *IEEE Trans. MTT*, 47(6), 769-774, 1999.

[7] C.L. Holloway, *Microwave and Optical Techn. Lett.*, 25(3) 162-168, 2000.

[8] M.E. Goldfarb and A. Platzker, *IEEE Trans. on MTT*, 38(12), 1957-1963, 1990.

[9] Y. Taguchi, K. Miyauchi, K. Eda, and T. Ishida, *IEEE MTT-S Dig.*, June, 1325-1328, 1993.

[10] W. Heinrich, *IEEE Trans. on MTT*, 38(10), 1468-1472, 1990.

[11] C.L. Holloway and G.A. Hufford, *IEEE Trans. on EMC*, 39(2), 73-78, 1997.

[12] C.L. Holloway and E.F. Kuester, *IEEE Trans. on MTT*, 43(5), 1204-1208, 1995.

[13] R.K. Hoffmann, *Handbook of Microwave Integrated Circuits*. Norwood, MA: Artech House, Inc., 1987, 116-117.

[14] B.C. Wadell, *Transmission Line Design Handbook*. Norwood, MA: Artech House, Inc, 1991, 125-137.

[15] G.H. Owyang and T.T. Wu, *IRE Trans. Antennas and Propag.*, 6, 49-55, 1958.

[16] S.B. Cohn, *Trans. of the IRE*, 2, 52-57, 1954.

[17] E.F. Kuester, *IEEE Trans. MTT*, 32(1), 131-133, 1984.

[18] R.B. Marks and D.F. Williams, *NEPCON East*, Boston, June 13-16, 1994.

[19] N. Morgan and D. Walker, NIST, Boulder, CO., personal communication.